AD-A127 269 DEMONSTRATION OF SQUID (SUPERCONDUCTING QUANTUM INTERFERENCE DEVICE) PARA..(U) TRW SPACE AND TECHNOLOGY GROUP REDONDO BEACH CA APPLIED TECHN.. A H SILVER 1/ 1

UNCLASSIFIED NOV 82 N00014-81-C-2495 F/G 9/5 NL

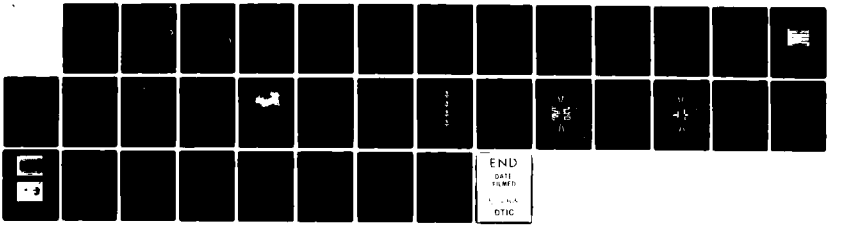

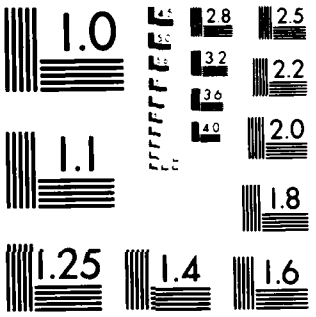

TRW Space & Technology Group
One Space Park
Redondo Beach, CA 90278
213 535 4321



ANNUAL PROGRESS REPORT

TO THE

NAVAL RESEARCH LABORATORY
CODE 6854
4555 OVERLOOK AVE., S.W.
WASHINGTON, DC 20375



ON

# DEMONSTRATION OF SQUID PARAMETRIC AMPLIFIER

CONTRACT NO. N00014-81-C-2495
SEPTEMBER 1981 - SEPTEMBER 1982

PREPARED BY

A.H. SILVER
ADVANCED PRODUCTS LABORATORY
APPLIED TECHNOLOGY DIVISION
TRW

NOVEMBER 1982

TRW Inc.
Electronics &
Defense Sector

One Space Park
Redondo Beach, CA 90278
213 535 4321

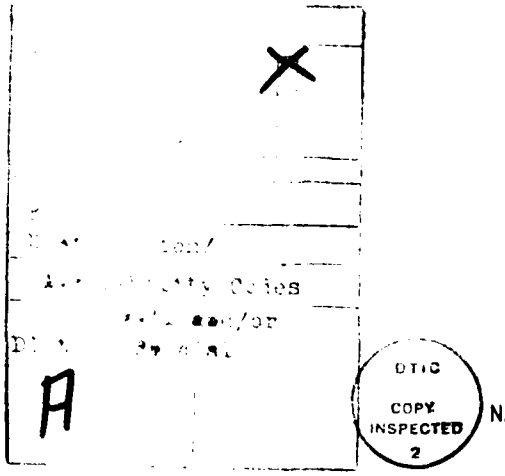


ANNUAL PROGRESS REPORT

TO THE

NAVAL RESEARCH LABORATORY
CODE 6854
4555 OVERLOOK AVE., S.W.
WASHINGTON, DC 20375

ON


# DEMONSTRATION OF SQUID PARAMETRIC AMPLIFIER

CONTRACT NO. N00014-81-C-2495
SEPTEMBER 1981 - SEPTEMBER 1982

PREPARED BY

A.H. SILVER
ADVANCED PRODUCTS LABORATORY
APPLIED TECHNOLOGY DIVISION
TRW

NOVEMBER 1982

UNCLASSIFIED

SECURITY CLASSIFICATION OF THIS PAGE (When Data Entered)

| REPORT DOCUMENTATION PAGE | | READ INSTRUCTIONS BEFORE COMPLETING FORM |
|---|---|---|
| 1. REPORT NUMBER | 2. GOVT ACCESSION NO. AD A127269 | 3. RECIPIENT'S CATALOG NUMBER |
| 4. TITLE (and Subtitle) Demonstration of SQUID Parametric Amplifier | | 5. TYPE OF REPORT & PERIOD COVERED Annual Report Sept. 1981 to Sept. 1982 |
| | | 6. PERFORMING ORG. REPORT NUMBER |
| 7. AUTHOR(s) A. H. Silver | | 8. CONTRACT OR GRANT NUMBER(s) N00014-81-C-2495 |
| 9. PERFORMING ORGANIZATION NAME AND ADDRESS Advanced Products Laboratory TRW Space and Technology Group One Space Park, Redondo Beach, CA 90278 | | 10. PROGRAM ELEMENT, PROJECT, TASK AREA & WORK UNIT NUMBERS P.E.62762N XF 62-584-004 |
| 11. CONTROLLING OFFICE NAME AND ADDRESS Naval Research Laboratory, Code 6854 4555 Overlook Avenue SW Washington DC 20375 | | 12. REPORT DATE November 1982 |
| | | 13. NUMBER OF PAGES 32 |
| 14. MONITORING AGENCY NAME & ADDRESS(if different from Controlling Office) | | 15. SECURITY CLASS. (of this report) Unclassified |
| | | 15a. DECLASSIFICATION DOWNGRADING SCHEDULE N/A |

16. DISTRIBUTION STATEMENT (of this Report)
Approved for Public Release
Unlimited Distribution

17. DISTRIBUTION STATEMENT (of the abstract entered in Block 20, if different from Report)

18. SUPPLEMENTARY NOTES

19. KEY WORDS (Continue on reverse side if necessary and identify by block number)
Parametric amplifier, low noise amplifier, microwave amplifier, Josephson junction, SQUID, array, monolithic superconducting transformer.

20. ABSTRACT (Continue on reverse side if necessary and identify by block number)
This is the first Annual Report of an effort to demonstrate a low noise superconducting microwave amplifier. The amplifier is a nearly degenerate, single idler parametric amplifier which uses the nonlinear inductance of a single junction SQUID (Superconducting QUantum Interference Device). The design frequency is 9 GHz, 10 dB gain, and 16% bandwidth. In order to maximize the saturation power, the device impedance was chosen near 1Ω and a matching network was designed to transform to 50Ω. In later designs, a

DD FORM 1 JAN 73 1473 EDITION OF 1 NOV 65 IS OBSOLETE

UNCLASSIFIED

SECURITY CLASSIFICATION OF THIS PAGE (When Data Entered)

TABLE OF CONTENTS

20. continued

coherent array of SQUIDs is expected to increase the power and impedance. This report includes the design and test of the 50Ω to 1Ω broadband transformer, design and fabrication of the SQUID amplifier, and both saturation and noise analyses of the single SQUID and SQUID array. The analytical results, reported to the 1982 Applied Superconductivity Conference are: the noise temperature of the single SQUID parametric amplifier is equal to the amplifier termination temperature $T_O$, the response is linear to several percent of the flux quantum energy in the SQUID: the amplifier will be saturated by broad band noise if the noise source temperature is much greater than 10 $T_O$; and the array parametric amplifier has the same noise temperature as the single device indicating an N-fold increase in dynamic range.

## LIST OF FIGURES

# I. INTRODUCTION

This is the Annual Progress Report for Contract No. N00014-81-C-2495, "Demonstration of SQUID Parametric Amplifier," covering the period from 14 September 1981 through 14 September 1982. The objectives of this project are the development and demonstration of a low noise SQUID microwave parametric amplifier. These objectives were met during this year by addressing SQUID amplifier design, circuit fabrication, measurements, and noise analysis.

## 2. WORK PLAN

This is a new contract for development and demonstration of a low noise Superconducting QUantum Interference Device (SQUID) parametric amplifier at microwave frequencies. The focus of this contract is the investigation and demonstration of a SQUID negative resistance amplifier at X-band. A SQUID array is then projected to increase the available power and operating impedance. The approach adopted utilizes monolithic superconducting integrated circuits which were designed, fabricated, and tested at TRW.

Three tasks were undertaken in the first year:

Task 1. Amplifier design and fabrication,

Task 2. Measurements,

Task 3. Noise analysis.

A number of the steps are very similar to those required for a contract with the Office of Naval Research, "Application of Josephson Junction SQUIDs and Arrays." Such steps are carried out jointly, and are reported to both agencies. TRW is also conducting Independent Research and Development on Advanced Josephson Devices. That research is principally concerned with developing Josephson integrated circuit fabrication capability. Some of the activities of that project impact on this contract and are discussed here.

## 3. PROGRESS

### 3.1 Transformer Design

Since the SQUID paramp is necessarily a very low impedance device, a suitable transformer is an essential ingredient for evaluating the basic device, particularly with respect to available power. In order to carry out this transformation in both impedance and dimension in a reproducible and predictable manner, the transformer is integrated with the active circuitry in a monolithic fashion.

The basic architecture of the transformer was presented in the contract proposal. We have refined the design for the TRW fabrication process and reconsidered the problems of launching from 50Ω coaxial cable into 50Ω coplanar line, dimensional step from 1 mm coplanar line at 50Ω, and construction of capacitors in the lumped element impedance transformer. The electrical design was optimized numerically using COMPACT with a computed VSWR < 1.25 over the 8-12 GHz band (Figure 1). Figure 2 shows the equivalent electrical circuit and the geometrical layout.

A test of the effect of changing dimensions in 50Ω coplanar line was performed by fabricating three 50Ω transmission lines: a continuous coplanar line at mm dimensions, a sharply stepped coplanar line, and a short, tapered transition as shown in Figure 3. The measured performance showed no significant differences between the three lines. Therefore, the input LC circuit in the transformer intended to tune out the inductance of the step in the coplanar line was deleted.

The transformer was designed to be fabricated on a 2 inch silicon wafer 0.015 in. thick with a minimum line width of 50μm. An OSM microwave launcher drives the 50Ω coplanar line which has a center conductor width equal to 1.3 mm, a ground plane spacing of 0.4 mm, and an effective dielectric constant of 4.4. The coplanar line is tapered at 50Ω to a center conductor width of 50μm, ground plane spacing of 30μm, and an effective dielectric constant of 6.4. The reduction in $\varepsilon$ and its

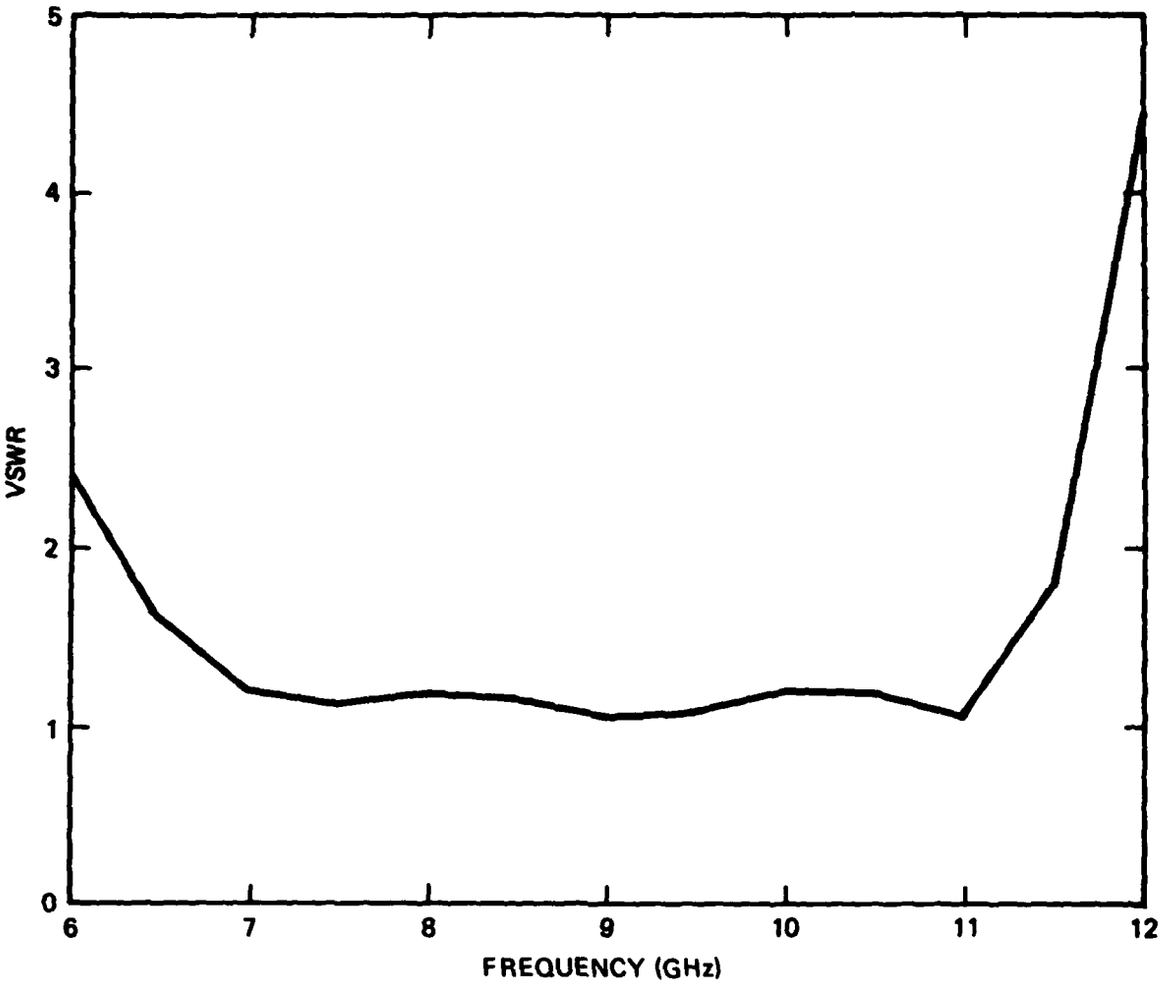


Figure 1. Computed VSWR of the optimized design of the 50Ω to 1Ω transformer.

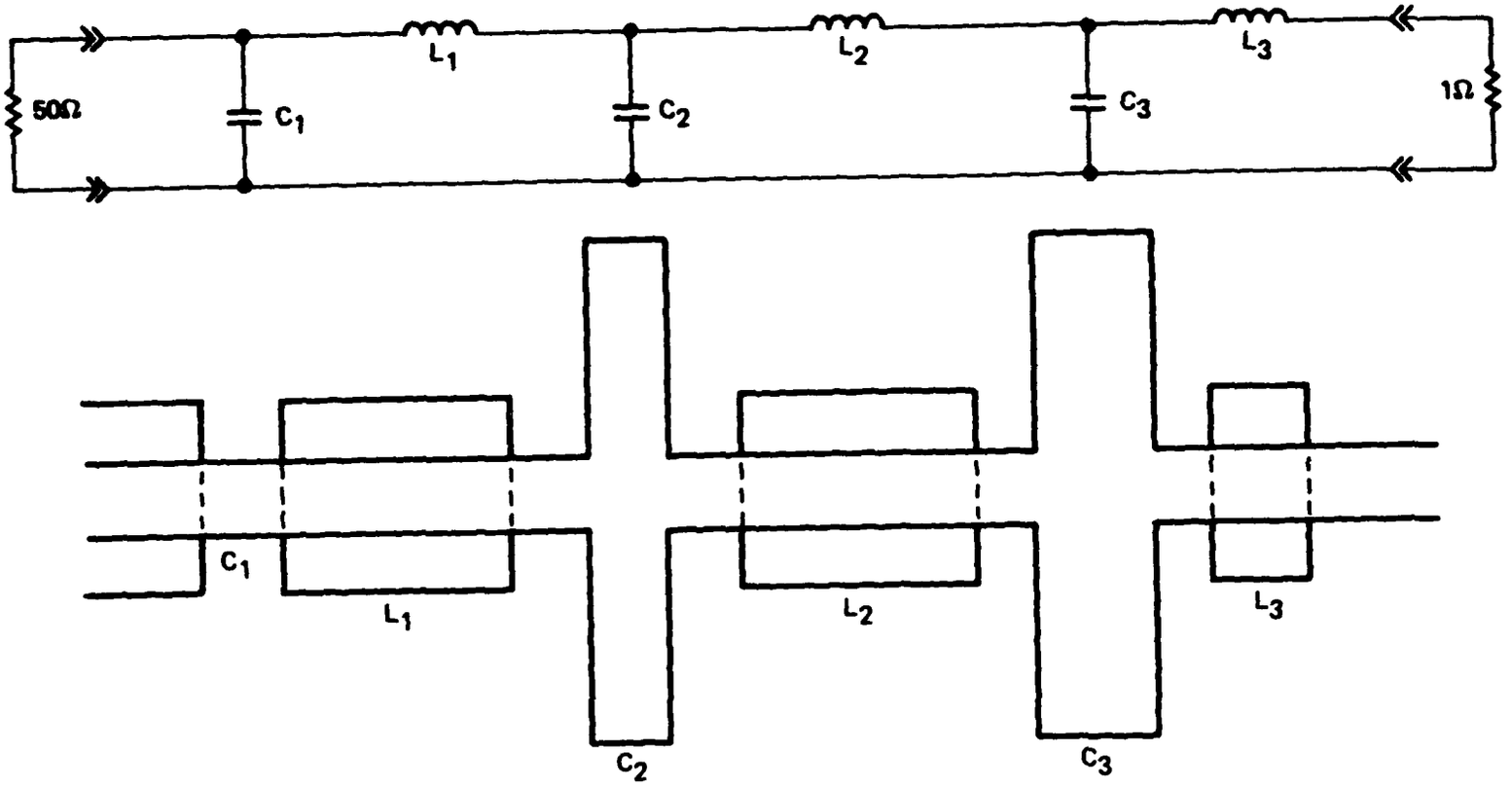


Figure 2. Equivalent circuit and el[illegible]d design of the 50Ω to 1Ω tr[illegible]sformer.

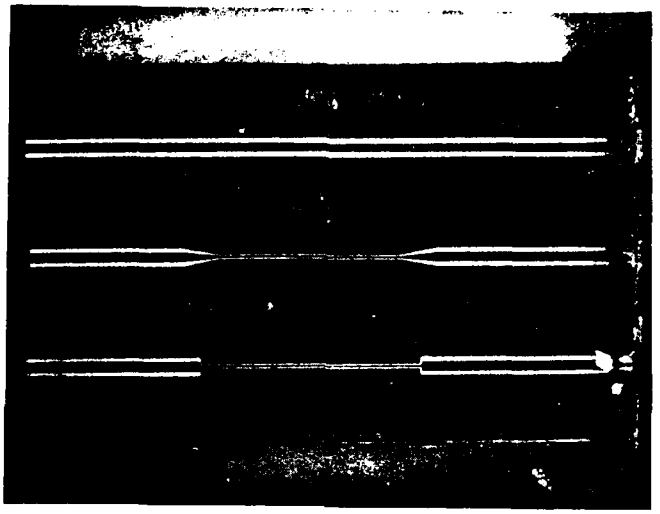

Figure 3. Photograph of the 50Ω coplanar lines used to test dimensional changes.

dependence on linewidth results from the finite thickness of the Si substrate. The 1Ω microstrip in the transformer is 50μm wide and separated from the Nb ground plane by 50nm $Nb_2O_5$ and 200 nm SiO. It has an effective $\varepsilon$=13.

The transformer design incorporates short (<$\lambda$/4) sections of coplanar and microstrip lines which act as lumped inductors and capacitors, respectively. The inductive lines are 50Ω coplanar lines terminated by 1Ω microstrip, with $L=Z_o\ell/v$, where $Z_o$ is the line impedance, $\ell$ the line length, and v the propagation velocity. Capacitors are 1Ω and 0.5Ω microstrip either terminated by 50Ω coplanar or used as open parallel stubs. The capacitance of short, open lines is given by $C=\ell/Z_o v$.

Photolithographic patterns were defined as 4-level masks and produced at the TRW Microelectronics Center for the combined dimensional and impedance transformer. For the dimensions and tolerances required, masks were fabricated directly at the reticle level in an Electromask pattern generator. Figure 4 shows the computer-generated composite of three 1 cm x 2 cm chips which will be fabricated on 2" silicon wafers, .015" thick. Each chip has 2 coplanar inputs with tapered lines. On one chip the reduced width coplanar line couples directly through; on the second chip, transformers from each end are connected for in-out transmission measurements. The third chip has each coplanar line and transformer terminated with a matched resistive load. Figure 5 is an expanded plot of the transformer and terminating resistor on the third chip.

The transformers were fabricated in a 1 cm x 2 cm format on 2" diameter silicon wafers with an insulating $SiO_2$ surface. Three test chips are produced on each wafer. Following fabrication, the wafer was cleaved with a modified Tempress scriber and the chips mounted in a holder suitable for connection to an OSM coaxial bulkhead launcher. Measurements are made at T=4K with an HP-8410 Network Analyzes. The data are in the form of the scattering matrix coefficients $S_{11}$ and $S_{12}$. Only the magnitude of S is reported since the phase is difficult to calibrate with long coaxial lines into the helium dewar.

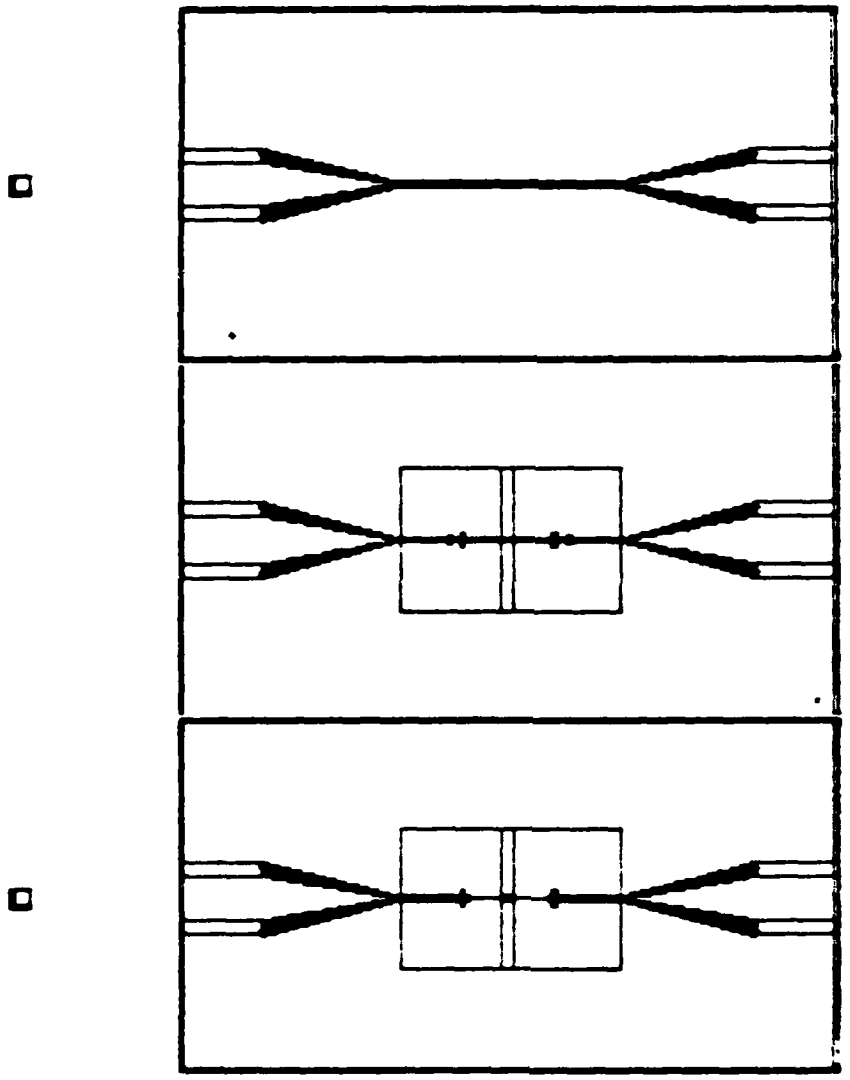

FIGURE 4. Printout of composite masks for the 50Ω to 1Ω transformers. Top: 50Ω stepped coplanar transmission lines; Center: 50Ω coplanar to 1Ω microstrip to 50Ω coplanar line; Bottom: 50Ω coplanar to 1Ω microstrip terminated.

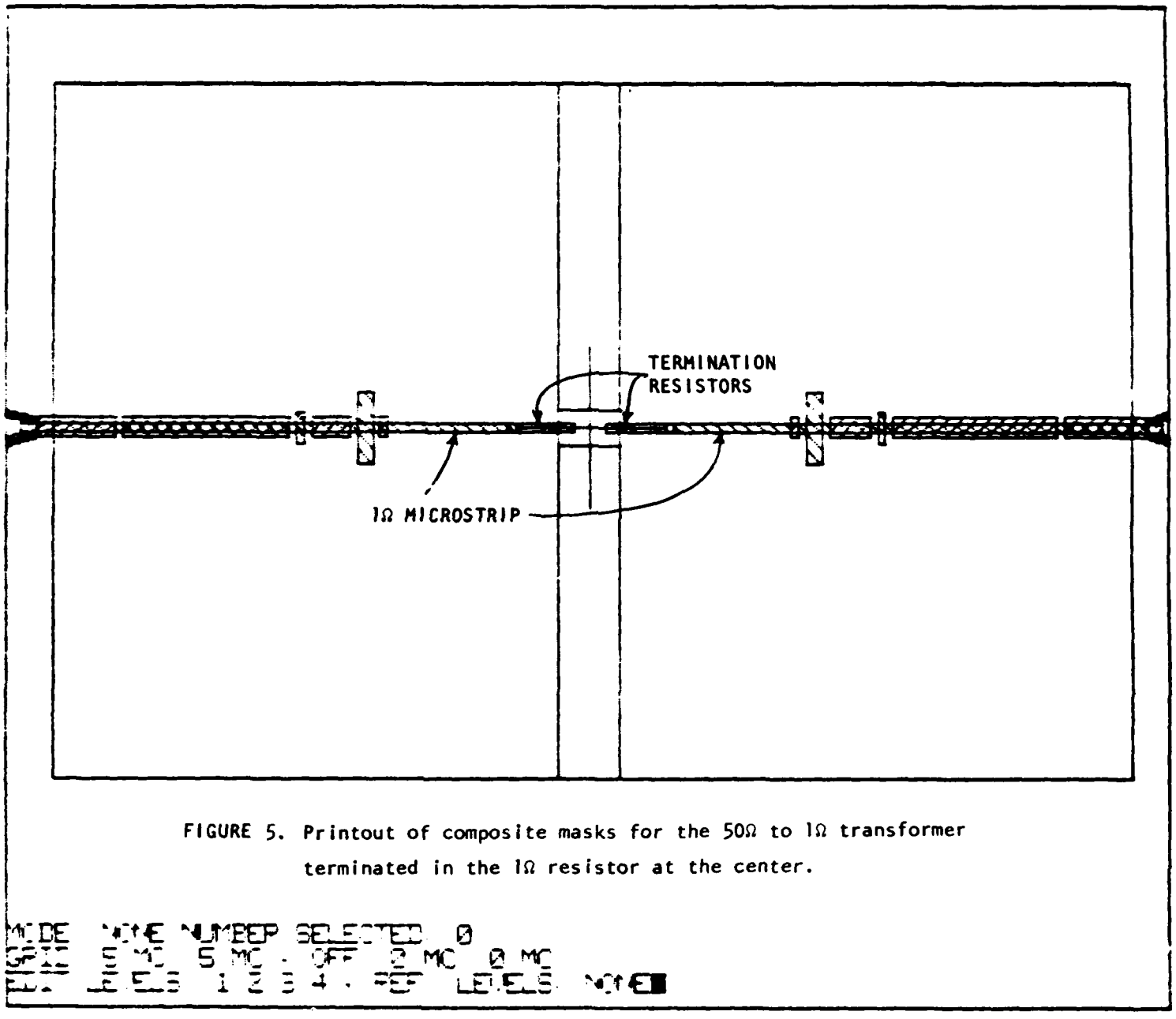


FIGURE 5. Printout of composite masks for the 50Ω to 1Ω transformer terminated in the 1Ω resistor at the center.

The test transformer chips are mounted with a coaxial connector at each end as shown in Figure 6. As anticipated, connecting the coplanar input to the bulkhead connector was a significant problem. An acceptable solution is to use In solder to connect gold ribbon from the connector center pin to the bulkhead to the coplanar lines. To facilitate soldering to the Nb film, a gold film is evaporated over the Nb. This is done before the Nb is patterned. Figure 7 shows the response of the simple tapered coplanar lines at 4 kelvin; Figure 8, the response of the double-ended transformer, in which the 50Ω coplanar line is transformed to 1Ω microstrip at the center of the chip, and then transformed back to 50Ω coplanar at the other end of the chip. We have not measured good S-parameter characteristics with the terminated transformers and we attribute this to a problem in making good contact with the resistors.

## 3.2 SQUID Amplifier

The first phase parametric amplifier is an rf SQUID biased at a phase of $\pi/2$ across the junction and driven by an 18GHz pump. The SQUID was designed to utilize the $Nb/Nb_2O_5/PbBi$ junctions used at TRW. The source impedance derived by $\sqrt{L/C}$ is set at 0.3Ω such that the 1Ω transformer load will result in Q=3. The design values are selected by setting the flux quantum energy $\approx 10^4 kT$, producing:

$L = 5pH$

$C = 65pF$

$\beta = 1$

$i_c = 67\mu A$

$j_o = 9A/cm^2$

Area = 50 um x 14.9 um = 745 $um^2$

Masks were produced at the TRW Microelectronics Center using an Applicon computer-aided-drafting system and an Electromask Pattern Generator. With the 50μm linewidths required, masks were produced directly at the reticle. Four amplifier chips were placed on each 2" diameter silicon wafer (1 cm x 2 cm format), encompassing two different amplifier configurations. Figure 9 is a computer generated composite

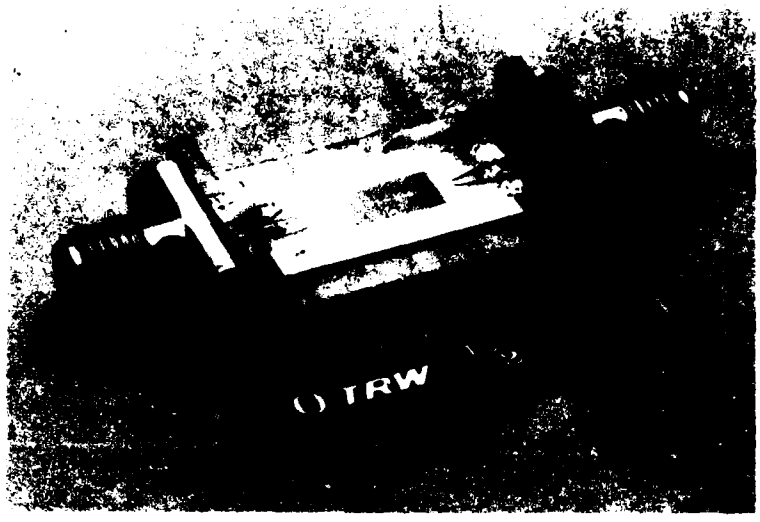


FIGURE 6. Photograph of transformer test chip mounted in a brass holder and connected to two OSM bulkhead connectors. The tapered coplanar lines at each end are visible in the photograph. The grey rectangle in the center of the chip is anodized Nb covered with SiO. The transformers are located in the same rectangle but are not clearly visible in the photograph.

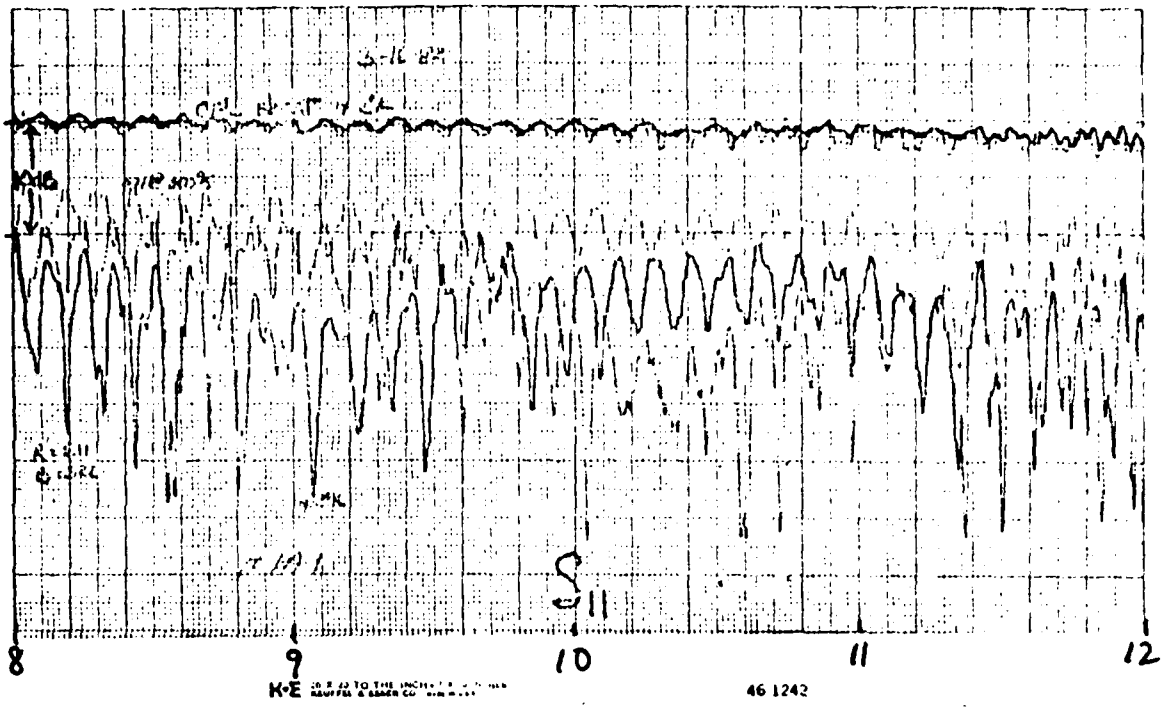


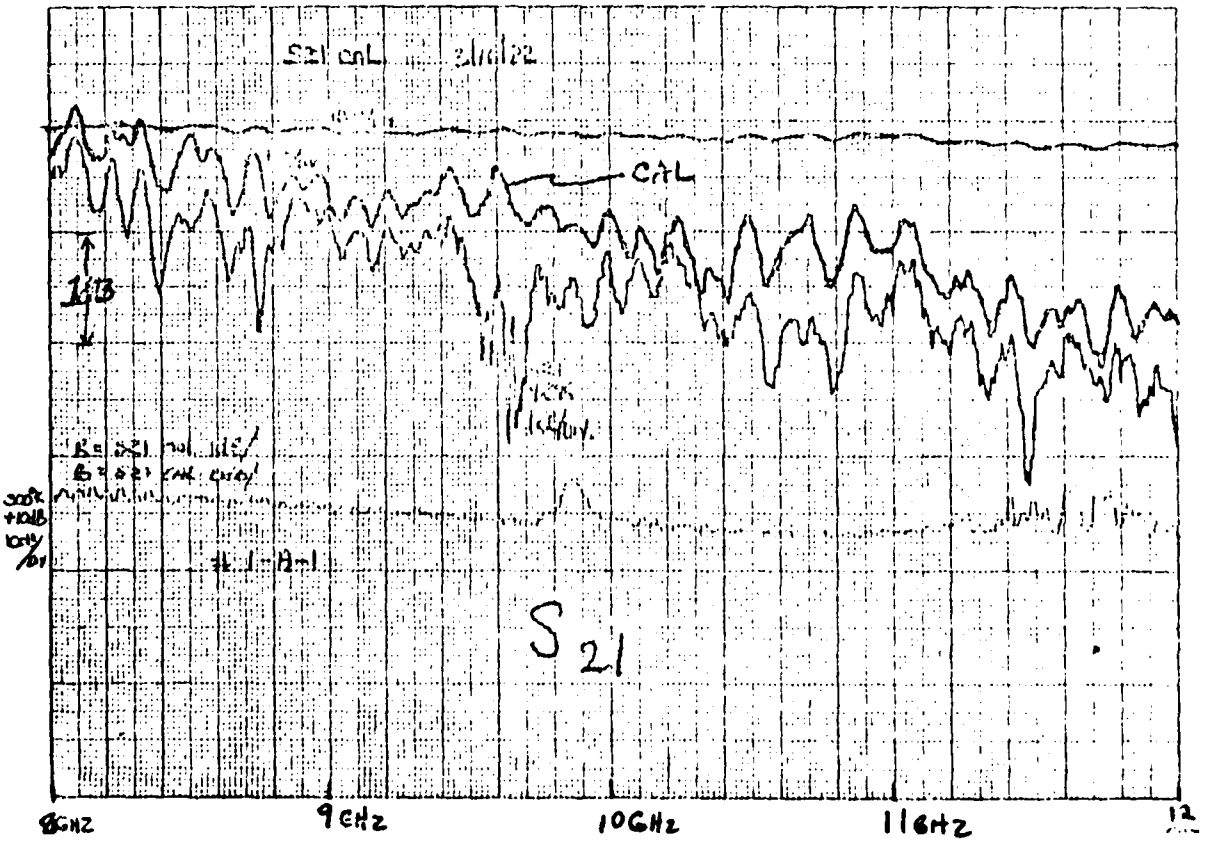


Figure 7. Response of 50Ω tapered coaxial lines on silicon substrate measured at 4K. The upper graph shows $S_{11}$ (and $S_{22}$) at 4K; the faint curve is $S_{11}$ at 300K. The lower graph is $S_{21}$ at 4K.

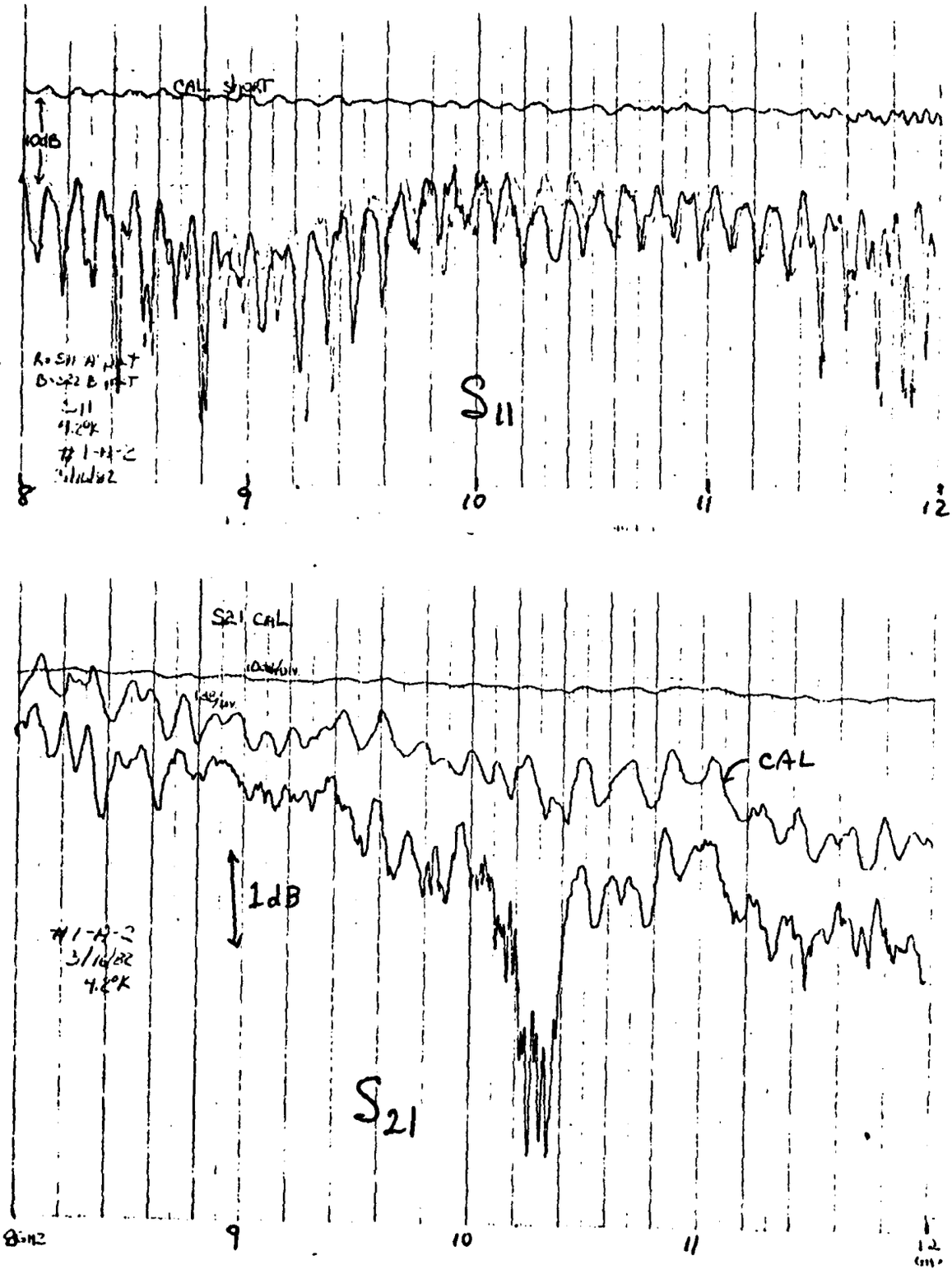


Figure 8. Response of the double-ended 50Ω to 1Ω transformers measured at 4K. The upper graph is $S_{11}$ (and $S_{22}$), the lower is $S_{21}$.

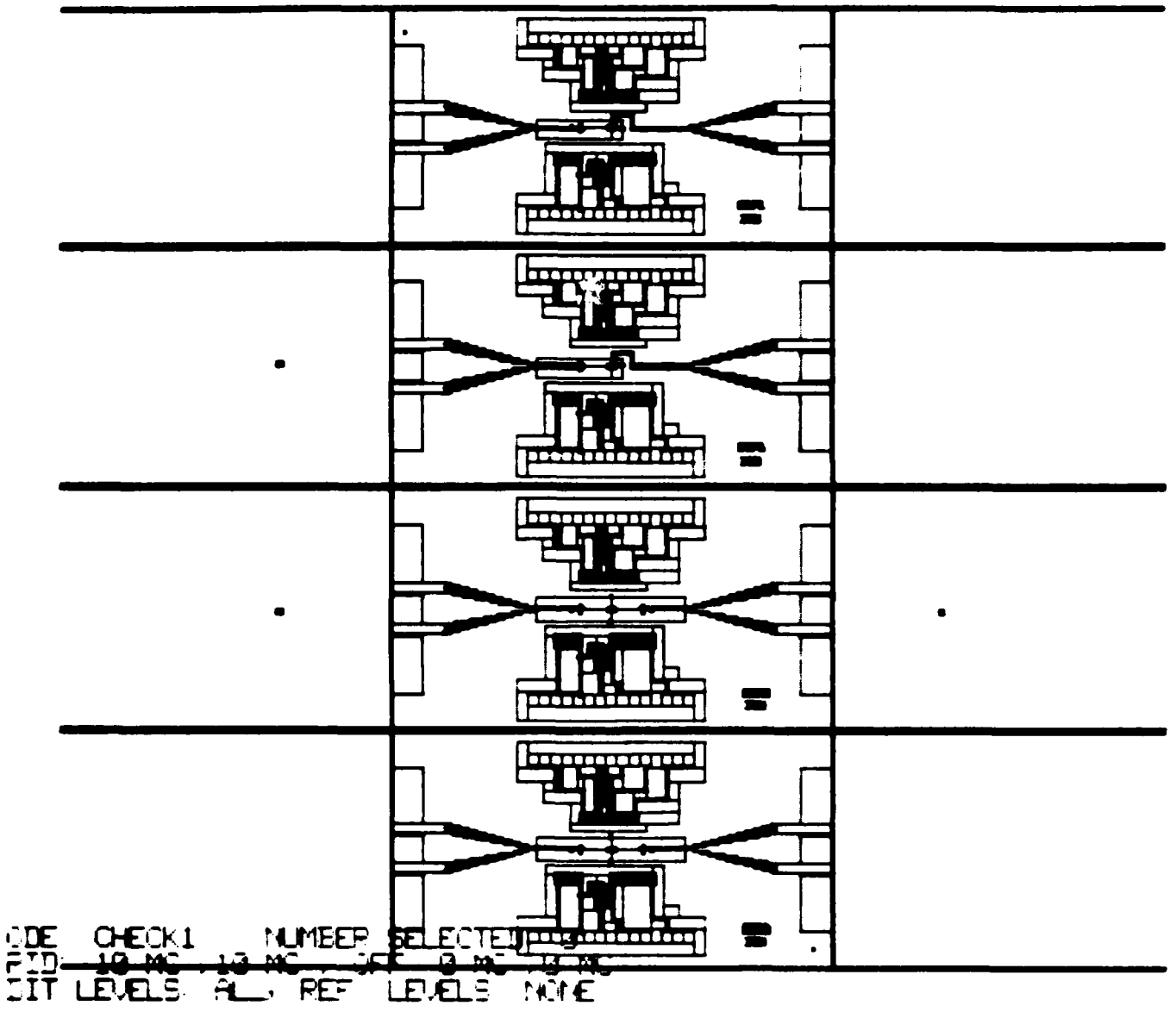


FIGURE 9. Layout of six masks on the two inch wafer. The upper two chips are amplifiers referred to as SQP1; the lower two chips are amplifiers SQP2.

of the multi-level mask set for the four-chip layout. Each chip contains two coplanar line inputs along the center line, and test junctions at the top and bottom of the chip.

Two different configurations of the amplifier were designed, SQP 1 and SQP 2. Figure 10 shows the enlarged layout of SQP 1. The transformer input to the SQUID is at the left; the pump input at the right. Figure 11 is an expanded plot of the six masks at the center of the chip, showing the impedance matched signal line at the left and mismatched pump line at the right. Both the microwave pump signal and the dc phase bias will be supplied by the coaxially fed pump line.

Figure 12 shows the layout of SQP 2. This chip is symmetric with two matching transformers (50Ω to 1Ω) connected symmetrically to the SQUID. The SQUID shown in Figure 13 is two inductive sections in parallel across the 1Ω microstripline. Since these inductors are the same as that of SQP 1, there is a reduction of L by a factor of two. To retain the same value of $\beta(=1)$ and resonance frequency, the junction area and hence $i_c$ and C are doubled. Also the Q is unchanged in this configuration. In this configuration we can operate the device as a transmission amplifier with a 3dB loss in gain. The pump signal is injected in one of the transformer inputs with a subsequent mismatch.

### 3.3 Fabrication

The amplifiers were fabricated on 2" silicon wafers using $Nb/Nb_2O_3/PbBi$ junctions and PbIn interconnect lines. Nb films deposited with our S-gun system exhibit $T_c > 9K$ and a residual resistance ratio $\simeq 4$. The junctions were fabricated by reactive-ion-oxidation followed by thermal PbBi deposition in the same vacuum system.

Significant problems with contact resistance and junction quality were encountered after the change from sapphire to silicon substrates. This was done to permit multi-chip fabrication and to eliminate photo-resist exposure problems at the edges of the substrate. Since silicon is more fragile than sapphire, samples were held in place in the vacuum system with vacuum grease rather than rigid clamping brackets for heat sinking and mechanical support. This tends to contaminate the front

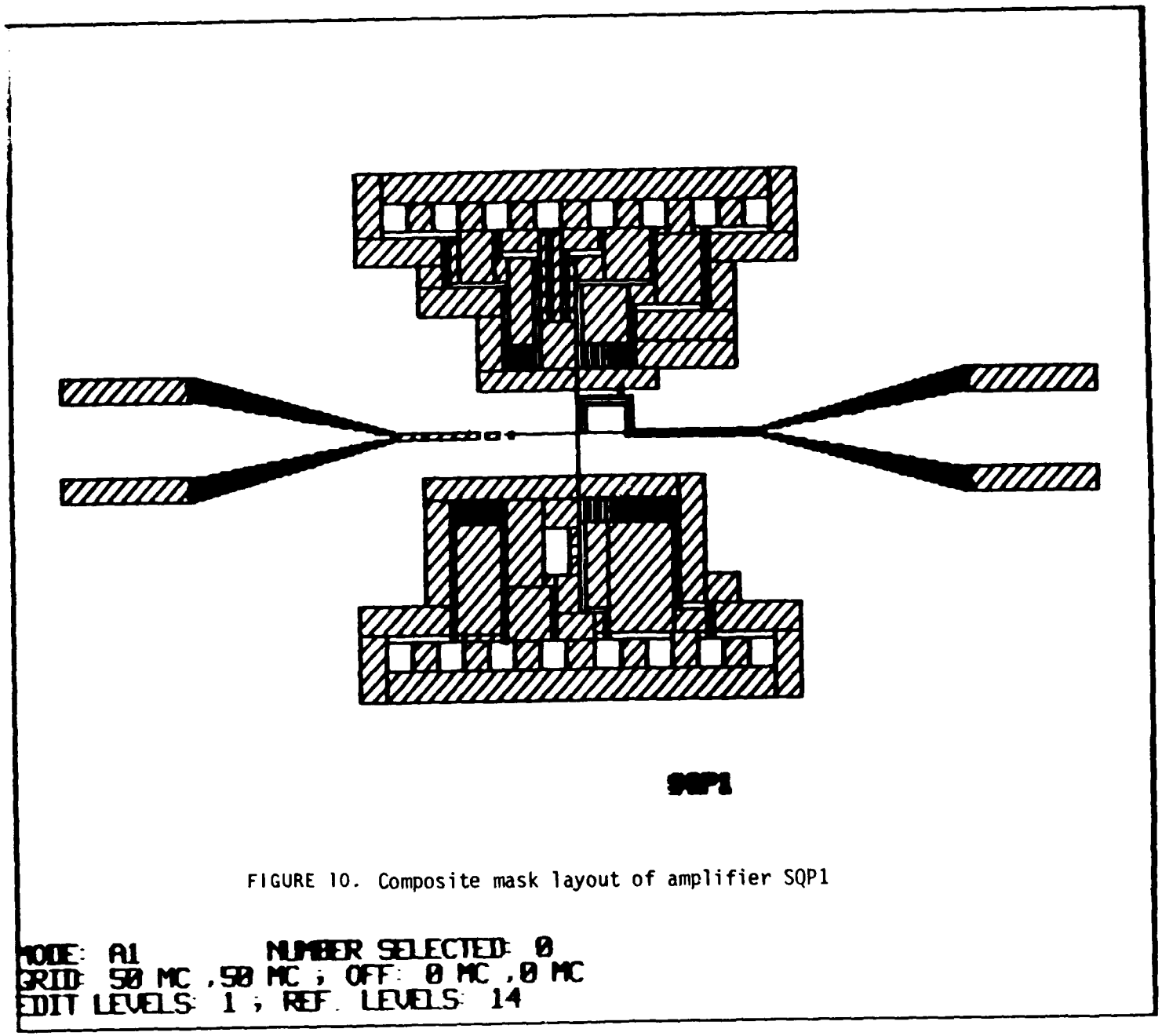


FIGURE 10. Composite mask layout of amplifier SQP1

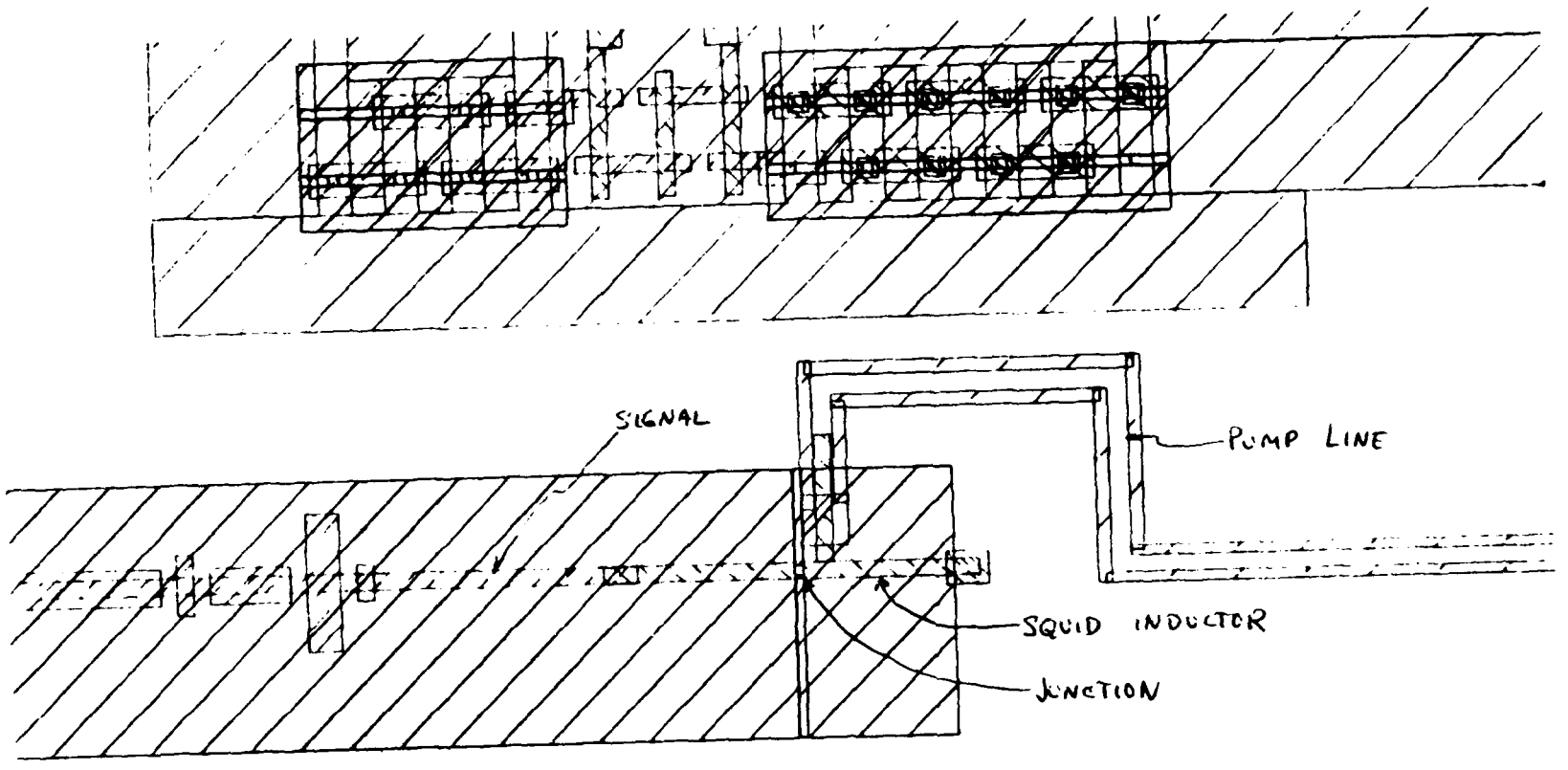


FIGURE 11. Expanded plot of the six composite masks of the SQUID amplifier SQP1.

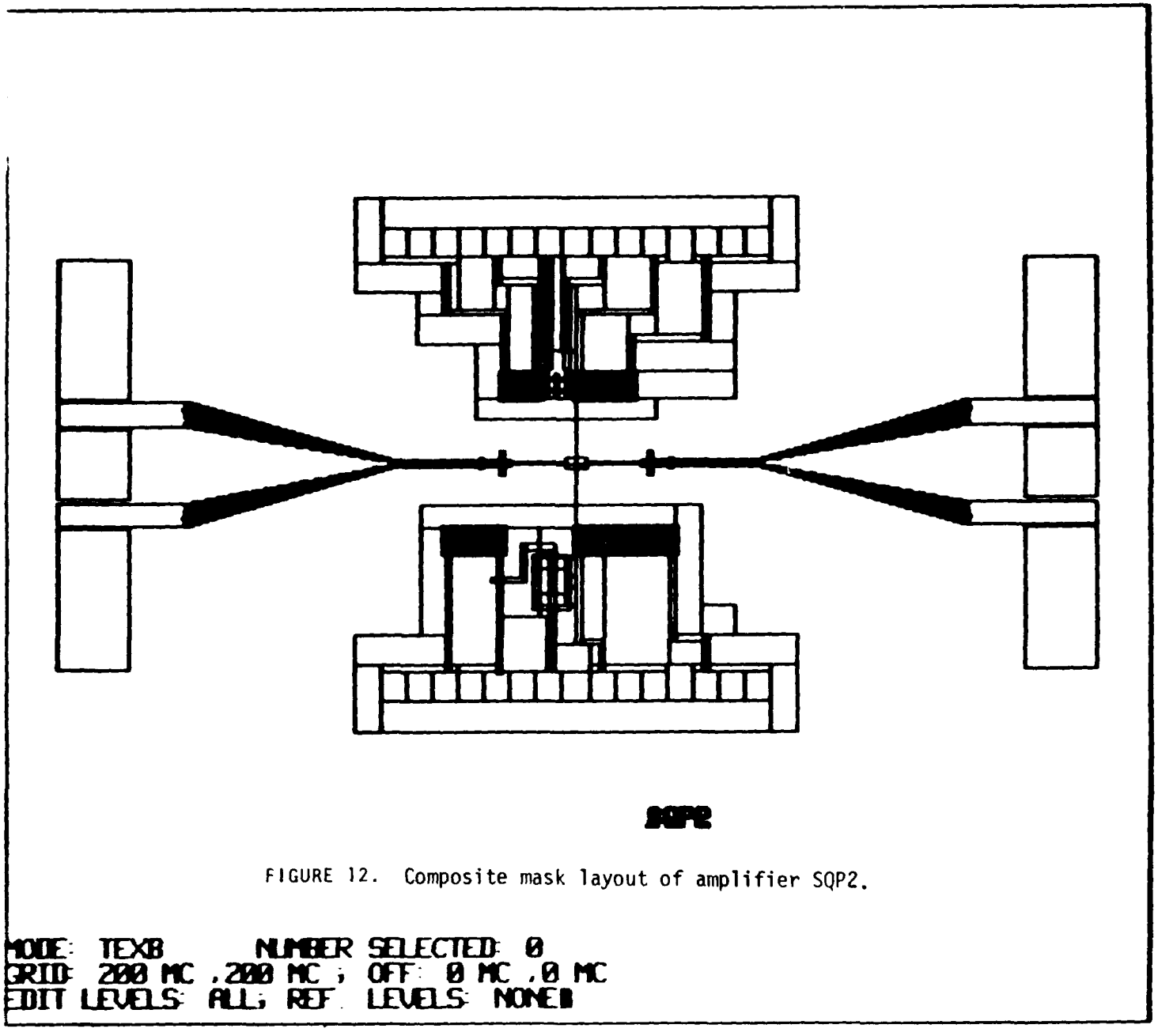


FIGURE 12. Composite mask layout of amplifier SQP2.

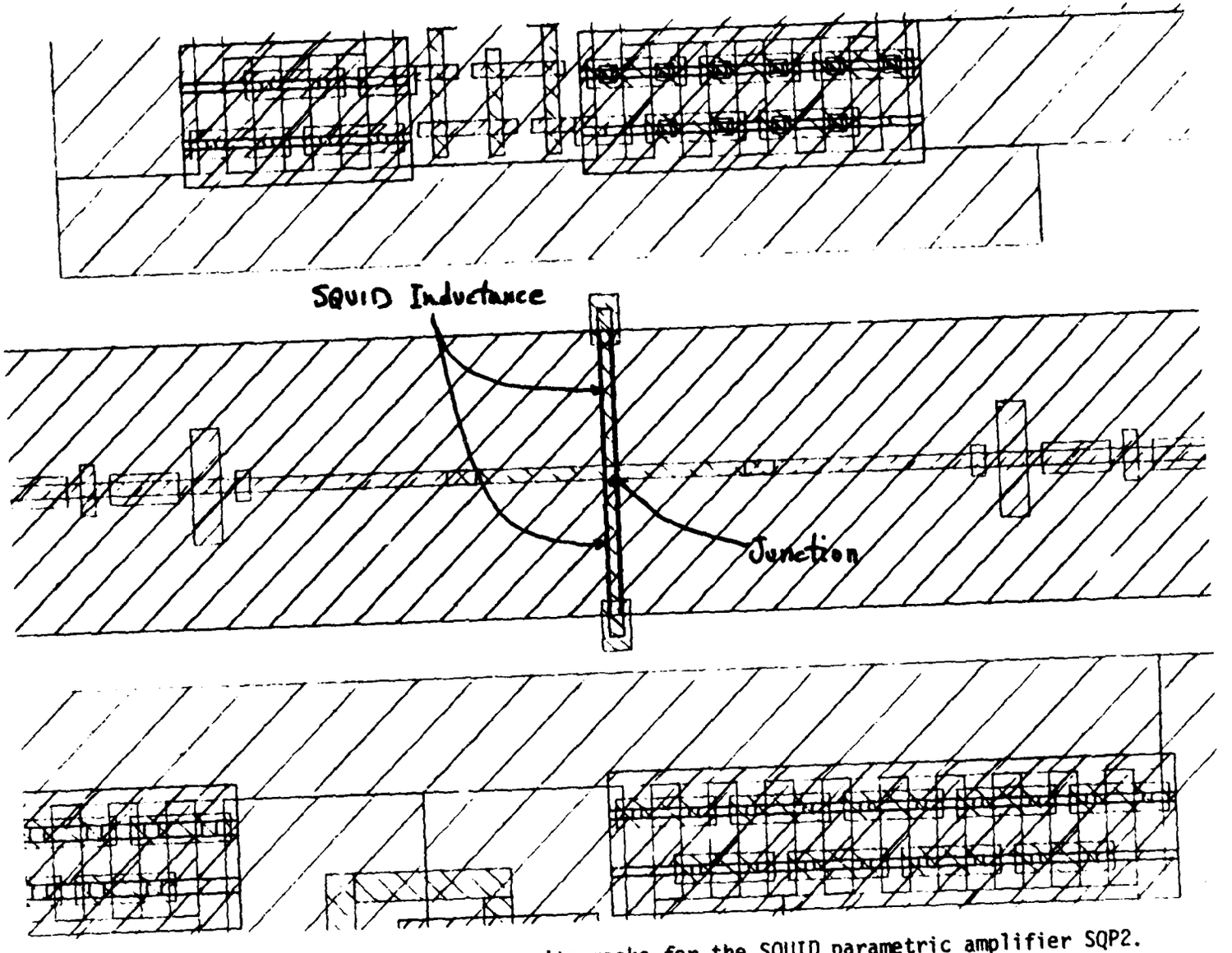


FIGURE 13. Expanded plot of the six composite masks for the SQUID parametric amplifier SQP2.

surface in the lift-off process following deposition. We have been successful at cleaning with hot xylene prior to the acetone lift-off, but a better solution is still being sought.

In addition, the lack of in vacuo surface cleaning just prior to deposition was judged to be another source of contamination. This was demonstrated by carrying out other depositions in the ion gun system. However, this approach is not a satisfactory solution since the vacuum system is not equipped for multiple component depositions, and the deposition of other than PbBi films contaminates the vacuum system for junction formation. Consequently, the general purpose e-beam evaporation system was modified under our IR&D program. This modification entailed installation of an rf sputtering system on which the substrates are mounted. In this configuration, the surfaces are sputter-cleaned prior to deposition. Also, the ion-gun system is prepared with a PbBi deposition prior to junction formation, providing a consistent background for reactive-ion-oxidation.

Figure 14 is a photograph of a SQUID paramp chip before mounting in the microwave test setup.

## 3.4 Analysis

Because of the eventual importance of the noise and saturation performance of the parametric amplifier in an array configuration, we have continued with numerical analysis of noise and dynamic range. This analysis will be reported at the 1982 Applied Superconductivity Conference and submitted for publication in the IEEE Transactions on Magnetics. A draft of that publication is attached.

The result of the calculations are: 1) the nearly degenerate SQUID paramp of the design developed here has a constant noise temperature $T_o$ equal to the device termination temperature; 2) the amplifier response is linear to several percent of the flux quantum energy; 3) the single SQUID paramp is easily saturated by broad-band noise if that noise temperature is much greater than $10T_o$; 4) the coherent SQUID array paramp

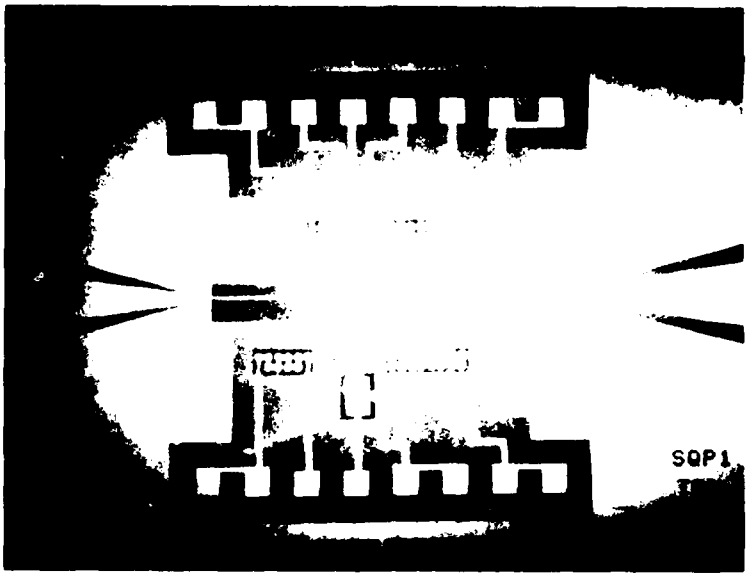


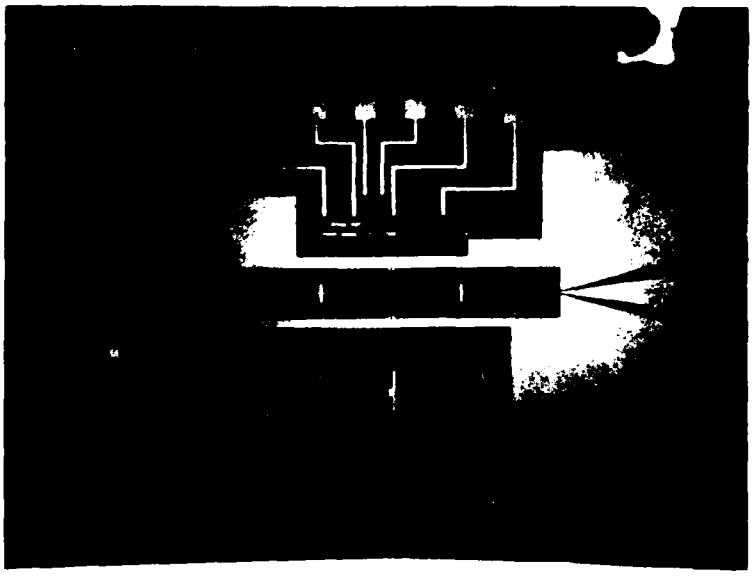

FIGURE 14. Photographs of the two different amplifier chips as fabricated on a silicon wafer. The field-of-view does not quite include the ends of the 2 cm long chips. The 9GHz SQUIDs are at the center of the chip with dc test structures at the top and bottom.

has the same noise temperature as the single SQUID parametric amplifier, indicating that the array of N SQUIDs will have a dynamic range N times that of the single device. Further details are included in the attached draft of "SQUID Parametric Amplifier,"

In conjunction with analysis of a resistive SQUID voltage-controlled-oscillator, we have observed that the resistive SQUID biased at $2\omega_o$, where $\omega_o$ is the SQUID LC resonance frequency, will oscillate almost exclusively at $\omega_J/2\ \omega_o$ for $\beta$=1 and Q>2. This can be viewed as a degenerate parametric oscillator similar to that predicted for the SQUID parametric amplifier if $Q_e J_1(Ap)>1$. Thus, it appeared very likely that a similar low noise amplifier could be operated with a self-pumped resistive SQUID. Very recently Calander, et al have reported such an experiment although in a non-degenerate form [J. Appl. Phys. 53, 5093 (1982)]. We have proposed to carry out specific analysis and measurements of this amplifier next year.

### 3.5 Measurements

Tests were made of several amplifiers at 9GHz using a cooled x-band circulator and an H-P Spectrum Analyzer as a receiver. No useful data was obtained, probably because of poor device quality as discussed above, and the poor noise figure of the SA. Just at the completion of this year, we received a NARDA low noise x-band GaAs FET amplifier to provide improved N.F. and also increase isolation from the SA. Measurements of new devices will proceed in the next quarter.

## 4. CONCLUSIONS

Several fabrication problems have been resolved and we expect to provide quantitative measurements next year. Analysis of noise and dynamic range of the single SQUID and SQUID array continue to indicate very useful application of the SQUID parametric amplifier.

APPENDIX A

# SQUID PARAMETRIC AMPLIFIER

A.H. Silver and R.D. Sandell*
TRW Space and Technology Group
One Space Park, Redondo Beach, CA 90278
J.P. Hurrell and D.C. Pridmore-Brown
The Aerospace Corporation
P.O. Box 92957, Los Angeles, CA 90009

## Abstract

The single junction SQUID was previously shown by analysis and simulation to be an attractive candidate for a parametric amplifier. Further calculations of the noise and saturation behavior of the nearly degenerate parametric amplifier have now been performed by numerical simulation. These simulations clearly show that the amplifier noise temperature will be approximately the device temperature $T_o$, and that the amplifier will be completely saturated in the presence of white noise characteristic of $3T_o$. Signal saturation of the amplifier also occurs for an output power $10^{-2}f_o\Phi_o^2/2L$, strongly limiting the dynamic range. However, a coherent array of N single junction SQUIDs is shown to have a signal saturation level increased by N relative to a single SQUID, with no increase in noise temperature, resulting in an N-fold improvement in dynamic range.

## Introduction

We have previously shown[1] that the single junction (or rf) SQUID is an attractive candidate for a single idler parametric amplifier in terms of gain, bandwidth, and phase stability. Furthermore, a specific linear array of tightly coupled SQUIDs was shown to support a stable mode identical to the single SQUID amplifier, but with power increased by N and impedance by N/2, where N is the number of SQUIDs in the array. The saturation and noise behavior of such amplifiers has now been computed and gives further support to the use of the SQUID as a low noise parametric amplifier.

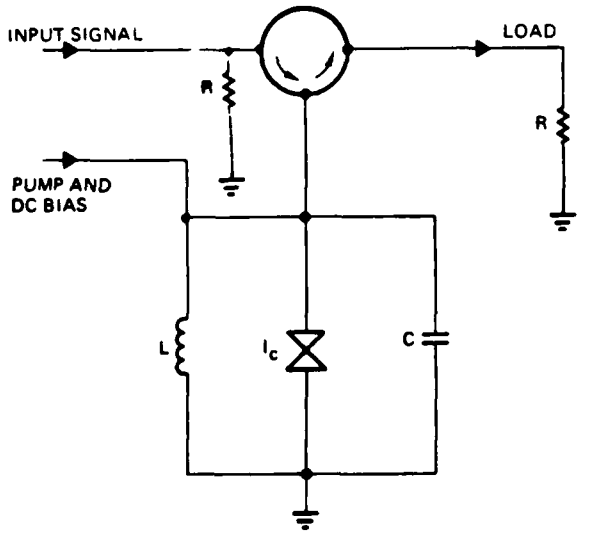


Figure 1. Equivalent circuit of the externally pumped SQUID parametric amplifier.

*Supported by the Naval Research Laboratory, Contract No. N00014-81-C-2495.

Manuscript received November 30, 1982

Consider the SQUID of Fig. 1 with inductance L and a Josephson tunneling junction with critical current $I_c$ and capacitance C. For frequencies well below the energy gap frequency, we neglect the internal quasiparticle resistance compared to the load resistance R. This configuration obeys the dimensionless equation

$$\ddot{\phi} + \eta\dot{\phi} + \beta\sin\phi + \phi = E(t)$$

where $\phi$ is the phase of the Josephson junction, $\beta = 2\pi LI_c/\Phi_o$, $\eta = \sqrt{L/C}/R$, time is measured in units of $\omega_o^{-1} = \sqrt{LC}$ and $E(t) = I(t)/I_c$ where

$$I(t) = I_o + I_s\cos\omega_s t + I_p\cos\omega_p t.$$

$I_o$, $I_s$, and $I_p$ represent dc bias, signal, and pump input currents. For $\beta=1$, $\eta<0.5$, an operating point set by $\theta = \pi/2$, and pumped at frequency $\omega_p = 2\omega_o$ with phase amplitude approximately $\pi/4$, the nearly degenerate SQUID parametric amplifier has high gain and a gain-bandwidth relation[1]

$$G(0)(\Delta\omega)^2 = \eta^2$$

Optimum bandwidth occurs for a loaded $Q = 1/\eta = 2$.

Successful performance of parametric amplifiers can be achieved by using circuit resonances to store idler power and thereby drive the system away from chaotic or marginally stable conditions. The bare Josephson tunnel junction exhibits a small signal plasma resonance which has been explored for superconducting amplifier operation[2]. No useful device, however, has resulted from either an unshunted single junction or multiple junctions. On the other hand, the low $\beta$, tunnel junction SQUID has a shunt inductance L and junction capacitance C which allow a well-defined, large signal resonance to occur. This same LC resonance can be preserved even in a large array of coupled SQUIDs[1]. This closely approximates the classical requirement for a successful amplifier. Furthermore, for the SQUID amplifier, $I_o$ in Eq. (2) is chosen to bias the junction phase $\theta$ at $\pi/2$ where the plasma frequency is identically zero. Therefore, the Josephson plasma resonance is not involved in the operation of this parametric amplifier.

## Saturation

The gain was previously[1] determined from both closed-form analysis and numerical simulations in the very small signal limit in the absence of noise. By increasing the signal amplitude in the computer simulation, the large signal response has now been calculated, providing estimates of both linearity and saturation. Calculations were performed for $\beta=1$ and $\eta=0.5$ with pump amplitudes $E_p=2.8$ and 3.2, corresponding to a small signal gain of 10 and 15 dB, respectively. Figure 2 shows the computed idler power as a function of input signal power for signal frequency at $1.05f_o$ ($E_p=2.8$) and $1.025f_o$ ($E_p=3.2$) with no noise added. The normalization of the signal input and idler power is $nf_okT_o$, where $f_o=\omega_o/2\pi$ and

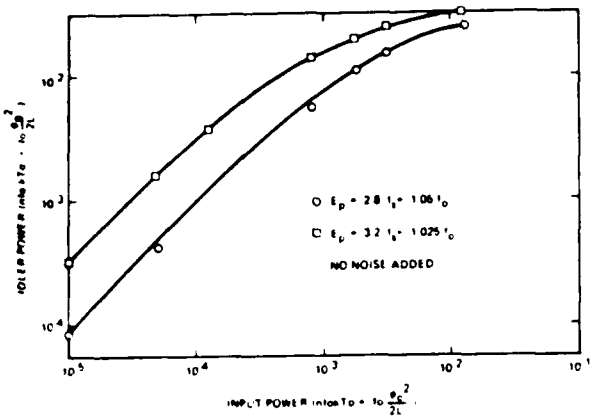


Figure 2. Computed idler response as a function of the input signal for two values of the pump level and amplifier gain, $E_p$=2.8 (10dB), and $E_p$=3.2 (15db). The power is normalized by $nf_o kT_o$, where $nkT_o$ is equal to the flux quantum energy and $f_o$ is the resonance frequency of the LC circuit.

$nkT_o=\phi_o^2/2L$, the energy of one flux quantum in the SQUID inductance, and $T_o$ is the operating temperature of the SQUID. SQUID amplifiers fabricated in a thin film format can have $L\leq 5\times10^{-12}$H, corresponding to $n\geq10^4$. In both cases plotted in Fig. 2, gain compression of 1dB occurs at an idler power $\approx 10^{-2}$ $nf_o kT_o$ or $10^{-2}f_o\phi_o^2/2L$. Strong saturation in the idler output sets in about $3\times10^{-2}f_o\phi_o^2/2L$. We point out that the idler power is used to test gain compression because the computed signal power in a two terminal device includes both the input and output powers. Frequency separation of the nearly degenerate idler makes the gain computation more straightforward.

Strong saturation near an output power of $3\times10^{-2}f_o\phi_o^2/2L$ is expected on the basis of the flux modulation model of the SQUID. One expects strong saturation in output power below the level of the pump power computed as $f_o\phi_p^2/L$, where $\phi_p$ is the amplitude of oscillatory flux in the SQUID at the pump frequency. The maximum value of $\phi_p$ for a well designed amplifier with $\beta=1$ is $\phi_{p,max}=\phi_o/2$; more appropriate values are $\phi_o/6$. Thus, strong saturation is expected below $(f_o\phi_o^2/2L)/36$, in good agreement with the results in Fig. 2.

## Noise

In practice, the noise performance will determine if these gains can be realized and over what bandwidth a useful dynamic range can be sustained. The added noise temperature of a classical, nearly-degenerate, high gain parametric amplifier is that of the idler termination. While the SQUID parametric amplifier obeys the classical equations at very small signals, the nonlinearities in the system make it necessary to determine the noise response for a wideband amplifier. We have performed a classical noise calculation to determine the contribution of potential noise sources such as pump noise[3] or up-conversion noise from near dc. Pump noise is expected to be minimized if the pump amplitude is such that $J_1(A_p)$ is near its maximum value, where $A_p$ is the fundamental component of the phase response to the pump[1]. Upconversion from very low frequencies should be ineffective since the resulting idlers are far from the signal band.

The calculation was performed by adding a Johnson noise generator in the load resistance R. This has the effect of adding broadband noise at both signal and idler ports of the paramp simultaneously. The Bachelier-Wiener[4] process was used to simulate the noise with discrete time intervals $\tau$, such that the cutoff frequency $\omega_c=1/2\tau=3.2\omega_o$. It is anticipated that this noise bandwidth will include all significant noise frequencies. The noise process is generated by a random walk in the phase $\theta$, which has a Gaussian distribution of time increments with variance $\sigma^2$, where

$$(\phi_o/2\pi)^2\sigma^2 = 4kT_oR\tau. \qquad (4)$$

Figure 3 displays the computed output temperature as a function of T for the same two amplifier conditions used in determining the gain saturation, $E_p$=2.8(10dB) and $E_p$=3.2(15dB). Similar to the scale in Fig. 2, the unit of temperature measurement, $10^{-4}nT_o$, relates temperature to the flux quantum energy via $nT_o=\phi_o^2/2Lk$. The calculated output noise temperature for small input temperature indicates that the classical result, $2T_o$ x gain, is approximately achieved. However, saturation of the output temperature and associated bright line gain compression exceed that anticipated by the idler performance shown in Fig. 2. A comparison of the integrated broadband output power to the narrowband idler/signal power indicates that broadband noise can more easily saturate the amplifier.

Based on the results shown above, the single SQUID is a low noise amplifier with useful but limited dynamic range which is potentially susceptible to broadband noise saturation. The utility of a SQUID array[1] to increase the total operating power and make impedance matching easier would be limited if the output noise power scales with the number of SQUIDs as does the signal power. Therefore, we have performed a noise calculation on the array similar to that for the single SQUID. In calculations and simulations on the array performance, each SQUID is assumed to be loaded with a resistance R. An independent Johnson noise generator with the same cutoff frequency $3.2\omega_o$ and other characteristics as that used for the single SQUID was added to each resistor. Thus, each SQUID is independently excited by thermal noise. From the array point-of-view, the uniform mode of the amplifier[1] is excited as well as all other modes which lie below the cutoff frequency. As a result, the signal and idler ports are correctly excited by noise if the end effects are neglected. Thus, the response to the effects of the bath temperature are adequately simulated, although

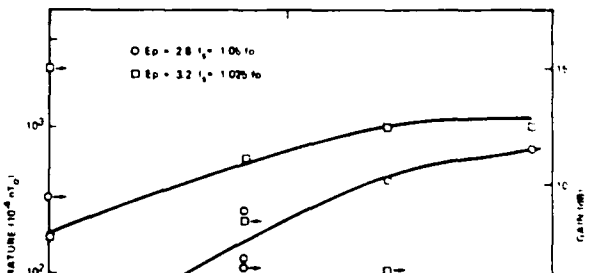


Figure 3. Computed output noise temperature of the SQUID parametric amplifier as a function of the input noise temperature for the same two pump (gain) conditions as shown in Fig. 2. Noise temperatures are normalized by $10^{-4}nT_o$, where n is the ratio of the flux quantum energy to $kT_o$.

TABLE I

COMPUTED NOISE RESPONSE OF THE SQUID ARRAY PARAMETRIC AMPLIFIER

The output noise temperature for 4, 16, and 32 SQUIDs normalized to that of a single SQUID for the same pump level and input noise temperature.

| PUMP LEVEL | INPUT NOISE TEMPERATURE ($10^{-4}nT_o$) | OUTPUT NOISE TEMPERATURE | | |
|---|---|---|---|---|
| | | 4 JUNCTIONS | 16 JUNCTIONS | 32 JUNCTIONS |
| $E_p$ = 2.8 10 dB GAIN | 1 | 1.8 | 1.5 | X |
| | 6.6 | 1.4 | 1.2 | 1.2 |
| | 26.4 | 1.7 | 2.1 | X |
| | 106 | 1.3 | 2.5 | X |
| $E_p$ = 3.2 15 dB GAIN | 1 | 0.8 | 0.6 | 0.9 |
| | 6.6 | 1.8 | 1.4 | X |
| | 26.4 | X | 3.4 | X |
| | 106 | X | 2.9 | X |

it is not an accurate representation of a broadband signal. The latter distinction does not exist for the single SQUID.

Table I summarizes the calculated output temperatures for arrays of 4, 16, and 32 junctions. The results, normalized to the single SQUID case, clearly demonstrate that, in the linear response range of input temperatures, the SQUID arrays exhibit no excess noise over that for the single SQUID. At the higher temperatures there is some evidence of noise increase. Scatter in the numbers in Table I reflects the accuracy of the noise calculations rather than significant variations.

This result means that an array of N single junction SQUIDs, operated as a nearly degenerate, externally pumped parametric amplifier[1], will have the following specifications relative to the single SQUID paramp:

| | |
|---|---|
| Gain | = 1 |
| Bandwidth | = 1 |
| Impedance | = N/2 |
| Saturation Power | = N |
| Noise Temperature | = 1. |

Since the array responds only to noise in the uniform mode, the total noise power does not increase while the signal power saturation level increases as N. The excess noise temperature of the nearly degenerate array amplifier operating at 4 kelvin is 4K, assuming the amplifier load is also at 4 kelvin. However, the dynamic range is limited by saturation level of $10^{-2}Nnf_oKT_o$ and by a noise floor of $f_oKT_o$, with a resulting dynamic range equal to $10^{-2}Nn$. Reasonable values of the ratio n= (flux quantum energy/thermal energy) are about $10^4$, with a maximum value of $10^5$ set by the Josephson penetration length limit on junction size. The array size may be limited by uniformity of Josephson current density and lithography, by parasitic capacitance or stray fields, or by impractically high impedance. Certainly $N=10^2$-$10^3$ should be realizable. Thus, a dynamic range at least $10^4$, and possibly as high as $10^6$, can be contemplated at 10dB gain without addressing new problem areas. With the more conservative value of $10^4$, based on $n=10^4$, $N=10^2$, the output saturation power will be 0.6μW at 10GHz (6μW at 100GHz); at $10^6$, saturation power will be 60μW at 10GHz (600μW at 100GHz).

## Comments

One further note about related measurements on Josephson parametric amplifiers and chaotic behavior. The simulations reported here and in Ref. 1 show that the Josephson junction, when incorporated into a low β, low Q SQUID which resonates the junction capacitance with the SQUID inductance, has modes of operation which are predictable, non-chaotic, and respond linearly. However, at large excitations, the behavior clearly becomes nonlinear with strong saturation, subharmonic generation, and other unexpected effects. Calendar[5], et al have recently reported low noise temperatures (≈30K) for "shunted" Josephson tunnel junctions which were self-pumped via internally generated Josephson oscillations. These devices were in fact low inductance "resistive" SQUIDs with β -factors approximately 2 and 4 for the lowest noise amplifiers. These results strongly suggest that the externally pumped configuration proposed by us will perform as a low noise amplifier. Despite the suggestion of Calander[5], et al that the external pump is a source of noise rise in Josephson paramps, only circumstantial evidence is offered that this is the case. We suggest that low noise follows from the low β, low Q SQUID configuration. Analysis of the resistive SQUID oscillator[6] shows a variety of instabilities for even modest values of Q or β, including subharmonic generation and anharmonic oscillations. Not surprising, the general rule to avoid these instabilities appears to be $Q\beta<2$, similar to the requirement to avoid subharmonic generation in the externally pumped parametric amplifier[1]. Thus, the internally pumped amplifier should be qualitatively similar to the externally pumped device without flexibility in setting the pump level ,although avoiding the need for a separate oscillator and adjustment for both the oscillator level and the dc phase value. Furthermore, a method of generating an internally pumped SQUID array amplifier does not appear to be at hand.

## References


1. A.H. Silver, D.C. Pridmore-Brown, R.D. Sandell, and J.P. Hurrell, "Parametric Properties of SQUID Lattice Arrays," IEEE Trans. Magn. MAG-17, pp. 412-415 (1981).
2. S. Wahlsten, S. Rudner, and T. Claeson, "Arrays of Josephson Tunnel Junctions as Parametric Amplifiers," J. Appl. Phys. 49, pp. 4248-4263 (1978). N.F. Pedersen, "Zero-Voltage Nondegenerate Parametric Mode in Josephson Tunnel Junctions," J. Appl. Phys. 47, pp 696-699 (1976).
3. M.J. Feldman and M.T. Levinsen, "Theories of the Noise Rise in Josephson Paramps," IEEE Trans. Magn. MAG-17, pp. 834-837 (1981).
4. G.M. Jenkins and D.G. Watts, Spectral Analysis and Its Applications , Holden-Day, Inc. (1968).
5. N. Calander, T. Claeson and S. Rudner, "Shunted Josephson Tunnel Junctions: High Frequency, Self-Pumped Low Noise Amplifier," J. Appl. Phys. 53, pp. 5093-5193 (1962).
6. A.H. Silver, R.D. Sandell, and J.Z. Wilcox, "SQUID Voltage-Controlled-Oscillator," IEEE Trans. Magn., current issue.

DISTRIBUTION LIST
FOR
TECHNICAL REPORTS

CONTRACT NO. N00014-81-C-2495

| | |
|---|---|
| Dr. Martin N Nisenoff, Code 6854<br>COTR Contract No. N00014-81-C-2495<br>Naval Research Laboratory<br>4555 Overlook Avenue, S.W.<br>Washington, DC 20375 | 50 |
| Administrative Contracting Officer<br>Naval Research Laboratory<br>4555 Overlook Avenue, S.W.<br>Washington, DC 20375<br>Ref: Contract No. N00014-81-C-2495 | 1 |
| Director<br>Naval Research Laboratory<br>4555 Overlook Avenue, S.W.<br>Washington, DC 20375<br>Attn: Code 2627 | 6 |
| Defense Technical Information Center<br>Building 5<br>Cameron Station<br>Alexandria, VA 22314 | 12 |
| Mr. Edgar A. Edelsack<br>Code 414<br>Office of Naval Research<br>800 North Quincy Street<br>Arlington, VA 22217 | 1 |
| Dr. Fernand D. Bedard<br>Department of Defense<br>R03<br>Fort Meade, MD 20755 | 1 |
| Dr. Nancy K. Welker<br>Laboratory for Physical Sciences<br>4928 College Avenue<br>College Park, MD 20740 | 1 |
| Dr. Kenneth Davis, Code 6855<br>Naval Research Laboratory<br>4555 Overlook Avenue, SW<br>Washington, DC 20375 | 1 |
| Mr. Max N. Yoder<br>Code 414<br>Office of Naval Research<br>800 North Quincy Street<br>Arlington, VA 22217 | 1 |

Dr. James E. Zimmerman 1
Mail Stop 2137
National Bureau of Standards
325 S. Broadway
Boulder, CO 80302

Dr. Clark A. Hamilton 1
Room 2137
National Bureau of Standards
325 S. Broadway
Boulder, CO 80302

Mr. Ernest Stern 1
MIT-P-327
Lincoln Laboratory
P. O. Box 73
Lexington, MA 02173

Dr. Ted Van Duzer 1
Dept. of Electrical Engineering and Computer Science
University of California
Berkeley, CA 94270

TRW Documents Section 1
Technical Information Center (TIC)
Building S, Room 1930
One Space Park
Redondo Beach, CA 90278

END

DATE
FILMED

5 — 83

DTIC